Theoretical Uncertainty of Measurements Using Quantitative Polymerase Chain Reaction

Jean Peccoud* and Christine Jacob#
*TIMC-IMAG, Institut Albert Bonniot, Faculté de médecine de Grenoble, 38706 La Tronche cedex, and #Laboratoire de biométrie, Institut National pour la Recherche Agronomique, 78352 Jouy-en-Josas cedex, France

ABSTRACT Current quantitative polymerase chain reaction (PCR) protocols are only indicative of the quantity of a target sequence relative to a standard, because no means of estimating the amplification rate is yet available. The variability of PCR performed on isolated cells has already been reported by several authors, but it could not be extensively studied, because of lack of a system for doing kinetic data acquisition and of statistical methods suitable for analyzing this type of data. We used the branching process theory to simulate and analyze quantitative kinetic PCR data. We computed the probability distribution of the offspring of a single molecule. We demonstrated that the rate of amplification has a severe influence on the shape of this distribution. For high values of the amplification rate, the distribution has several maxima of probability. A single amplification trajectory is used to estimate the initial copy number of the target sequence as well as its confidence interval, provided that the amplification is done over more than 20 cycles. The consequence of possible molecular fluctuations in the early stage of amplification is that small copy numbers result in relatively larger intervals than large initial copy numbers. The confidence interval amplitude is the theoretical uncertainty of measurements using quantitative PCR. We expect these results to be applicable to the data produced by the next generation of thermocyclers for quantitative applications.

INTRODUCTION

To what extent can polymerase chain reaction (PCR) be quantitative? Considering the number of experiments that have been reported using quantitative PCR (Q-PCR) steps, this question may sound naive. Yet, the exponential growth of a DNA molecule population that undergoes a PCR amplification raises the question of possible concomitant amplification of fluctuations. A simple example can help to clarify this issue. Imagine a single target DNA sequence amplified under such conditions that the yield of the reaction is 80%. After the first cycle of amplification, the probability that two molecules will result is 80%, with a 20% probability of a single molecule remaining. Similarly, after n cycles of amplification, the total number of molecules is situated between 1 and 2^n. This extreme example is still quite realistic, because the possibility of amplifying a single DNA sequence has long been reported (Erlich et al., 1991; Li et al., 1988; Snabes et al., 1994; Cui et al., 1989; Zhang et al., 1992). It underlines the necessity of a suitable statistical treatment of Q-PCR data.

Quantitative analysis is now one major use of PCR (see Ferre et al., 1994, for a review). Q-PCR has been done in a variety of contexts, such as the study of gene expression (Singer-Sam et al., 1992; Wang et al., 1989) or monitoring the progress of a therapeutic protocol (Lion et al., 1993). It has been particularly valuable in providing estimates of virus load during HIV-1 infection (Semple et al., 1993; Piatak et al., 1993; Wood et al., 1993) and hepatitis C virus infections (Simmonds et al., 1990). A review of all of these topics can be found in Mullis et al. (1994).

Despite the generalized use of Q-PCR protocols in many fields of the biological sciences, theoretical work on Q-PCR has been very scarce so far. The ratio of the amount of amplified target sequence over a standard (either internal or external) has received considerable attention. In most papers, the amplification process has been modeled by a deterministic geometric series (Santagati et al., 1993; Wiesner et al., 1993; Raeymaekers, 1993, 1994; Shire, 1994). Nedelman conducted the most detailed theoretical analysis of Q-PCR protocols by introducing stochastic models (Nedelman et al., 1992a,b). He designed a very detailed branching process to compare the conditions in which the three main quantification methodologies (external control, internal control, kinetic data with no control) currently in use are valid.

Like Nedelman, we have used the branching process theory. We concentrated on Q-PCR based on a kinetic observation of the amplification, but instead of studying current practices, we propose a new strategy for analyzing this type of data. The amplification can be monitored by withdrawing aliquots of the reaction at regular intervals (Hoof et al., 1991; Wiesner et al., 1992). This is a very labor-intensive operation, however, which prevents its use on large numbers of samples. It can also lead to cross-contamination problems. It should also be noted that the steep temperature gradient near the thermocycler is very unfavorable for the sampling of a precise volume with the usual liquid handling devices. A more promising approach has been worked out by Higuchi. He used a video camera to monitor PCR conducted in the presence of ethidium bromide in 96-well microtiter plates (Higuchi et al., 1993).

Received for publication 24 July 1995 and in final form 22 March 1996.
Address reprint requests to Dr. Jean Peccoud, TIMC-IMAG/Institut Albert Bonniot, Faculté de médecine de Grenoble, 38706 La Tronche cedex, France. Tel.: +33-76-54-95-05; Fax: +33-76-54-95-55; E-mail: jean.peccoud@imag.fr.

0006-3495/96/07/101/08 $2.00

Several of the limitations of Q-PCR protocols can be overcome by statistical analysis of a data set collected during the amplification process. Q-PCR protocols rely on heavy standardization procedures that compare the amount of an amplified target sequence to the amount of a standard introduced either internally or externally in the assay. The standards are chosen to ensure similar rates of amplification for the standards and the targets. The sample often has to be split and amplified several times to compare the different amplifications to different concentrations of the standard. In this paper, we show that a good estimator of the amplification rate can be computed with a set of dynamical data collected during amplification. With this estimator, a second estimator of the initial copy number as well as its confidence interval can be computed.

These two estimators have been derived and characterized analytically. Details of this work will be published elsewhere (Jacob and Peccoud, 1996a,b). In this paper we investigate the numerical and computational consequences of these analytical results. Because these results are asymptotic, their approximate validity must be verified after a finite number of amplification cycles. Using Monte Carlo simulations, we show that the limits are reached when the number of cycles is greater than 20 (see Table 1 and Fig. 1). To proceed to the analysis of simulated data, the shape of the asymptotic distribution of probability of the normalized number of amplified molecules requires study. In Fig. 2 we show that this shape is dramatically affected by both the initial copy number of the target sequence and the amplification rate. This work provides some interesting indications about the inherent uncertainty of PCR-based quantification protocols, especially when the initial copy number is close to unity.

THEORETICAL RESULTS

At the molecular level, the yield of a chemical reaction is the probability of the molecule of committing itself to a reaction. When the size of the molecule population is large, the law of large numbers applies, leading to a deterministic behavior. A predictable fraction of the population reacts, and the fluctuations of this fraction size become negligible as the size of population tends to infinity, whereas in con-

TABLE 1 Mean value and dispersion of $\hat{m}_n$ and $\hat{N}_{0,n}$ over the 500 simulated trajectories

	Cycle	Mean	Range	SD	SE
			$\hat{m}$		
$N_0 = 1$ and $m = 1.6$	10	1.60006745307	6.36364×10^{-1}	6.75162×10^{-2}	3.01941×10^{-3}
	20	1.60022242210	6.56857×10^{-2}	6.72448×10^{-3}	3.00728×10^{-4}
	30	1.6000146802	4.92395×10^{-4}	6.40470×10^{-4}	2.86427×10^{-5}
$N_0 = 1000$ and $m = 1.6$	10	1.60018002150	1.09504×10^{-2}	1.92464×10^{-4}	8.60724×10^{-5}
	20	1.60000984656	1.05250×10^{-4}	1.77414×10^{-4}	7.93420×10^{-7}
	30	1.59999951734	1.02051×10^{-4}	1.78139×10^{-5}	7.96661×10^{-7}
$N_0 = 1$ and $m = 1.8$	10	1.80230389426	1.91090×10^{-1}	2.99130×10^{-2}	1.33775×10^{-4}
	20	1.80000741525	1.03504×10^{-2}	1.60504×10^{-4}	7.17796×10^{-5}
	30	1.80000928590	5.58308×10^{-4}	8.38251×10^{-5}	3.74877×10^{-6}
$N_0 = 1000$ and $m = 1.8$	10	1.80001843029	5.83452×10^{-4}	8.83768×10^{-4}	3.95233×10^{-5}
	20	1.80000314882	2.87236×10^{-4}	4.60407×10^{-5}	2.05900×10^{-6}
	30	1.80000003152	1.50043×10^{-5}	2.49009×10^{-6}	1.11360×10^{-7}
			$\hat{N}_0$		
$N_0 = 1$ and $m = 1.6$	10	1.10572121086	3.79481	6.15589×10^{-1}	2.75300×10^{-2}
$\sigma_\infty = 0.50$	20	1.04560248695	2.33701	5.00548×10^{-1}	2.23852×10^{-2}
	30	1.04315214802	2.42596	4.94096×10^{-1}	2.20966×10^{-2}
$N_0 = 1000$ and $m = 1.6$	10	999.080060658	1.17863×10^{-2}	1.93715×10^{-1}	8.66321×10^{-1}
$\sigma_\infty = 15.80$	20	1000.04500834	9.71133×10^{-1}	1.57246×10^{-1}	7.03226×10^{-1}
	30	1000.17263029	9.60037×10^{-1}	1.55971×10^{-1}	6.97523×10^{-1}
$N_0 = 1$ and $m = 1.8$	10	1.01795953945	1.80043	3.49498×10^{-1}	1.56300×10^{-2}
$\sigma_\infty = 0.33$	20	1.01621795726	1.42881	3.16478×10^{-1}	1.41533×10^{-2}
	30	1.01629097804	1.38254	3.16453×10^{-1}	1.41522×10^{-2}
$N_0 = 1000$ and $m = 1.8$	10	1000.05332664	6.53775×10^{-1}	1.12547×10^{-1}	5.03323×10^{-1}
$\sigma_\infty = 10.54$	20	1000.08766640	6.40454×10^{-1}	1.03921×10^{-1}	4.64749×10^{-1}
	30	1000.12338803	6.45903×10^{-1}	1.04219×10^{-1}	4.66081×10^{-1}

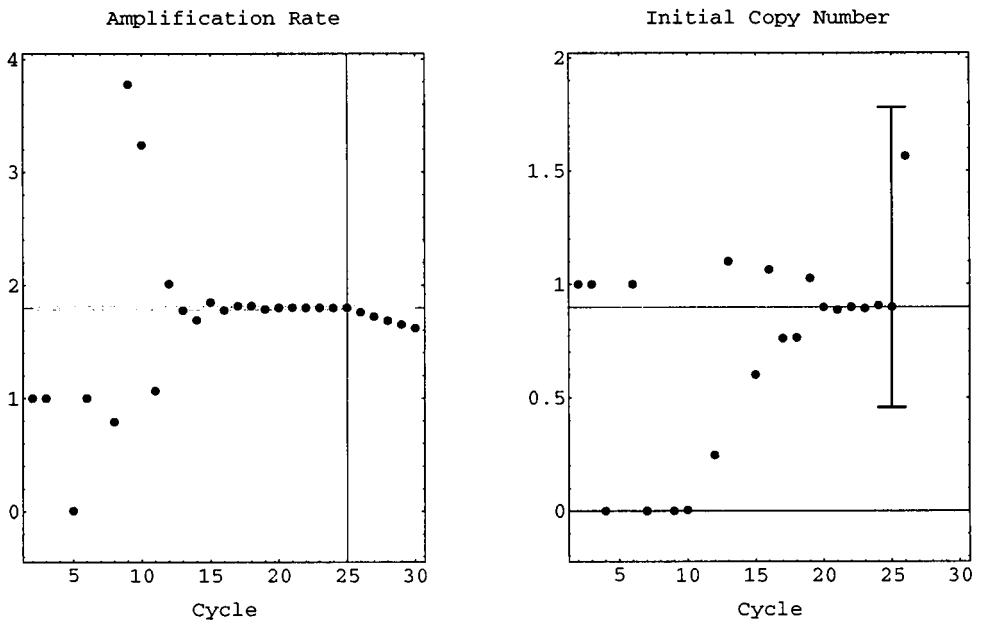

FIGURE 1 Statistical analysis of a PCR trajectory. The analysis of a data set simulating a PCR amplification is conducted in two steps. First, $\hat{m}_n$ is computed and plotted to verify its convergence and to determine the end of the exponential phase of the reaction materialized by the vertical line at cycle 25 on the left plot. Second, the series of $\hat{N}_{0,n}$ is plotted and the confidence interval is computed for the last cycle in the exponential phase. The parameter of this simulation was $m = 1.8$. The numerical values of these estimates are $\hat{m}_{25} = 1.7999$ and $\hat{N}_{0,25} = 0.89855$. One can notice that $\hat{m}_{25}$ is very close to 1.8, whereas $\hat{N}_{0,25}$ is stabilized below N_0.

trast, a small population size forces us to consider the probability of reaction for each molecule and the resulting stochastic behavior of the population (Erdi and Toth, 1989). The PCR is modeled by assuming that each DNA molecule can be duplicated not more than once with a probability p during a cycle of amplification. Thus p is also the yield of the reaction. The amplification rate of the reaction m is simply related to p, because $m = 1 + p$. The duplication of each molecule is assumed to be independent of the duplication of other molecules. This is a fair assumption, because PCR is usually conducted with an excess of reagents other than the DNA template, so that DNA molecules do not compete with each other for duplication. The number of molecules at the end of the nth cycle is denoted by N_n. N_0 is the initial number of molecules to be estimated. With these notations the series $\{N_n\}_{n \geq 0}$ fits with what is called a branching (or Galton-Watson) process in probability. Branching processes were first used to model the PCR for estimating the risk of false gene diagnosis resulting from replication errors of the *Taq* polymerase gene (Krawczak et al., 1989). Later on, they were also used by Nedelman to analyze the use of internal controls in Q-PCR experiments (Nedelman et al., 1992b), as well as most of the other current protocols of Q-PCR (Nedelman et al., 1992a).

The estimation of the mean value of the offspring distribution is a classical problem in branching process theory (Guttorp, 1991). In the case of PCR, the offspring mean is the rate of amplification, which can be estimated by

$$\hat{m}_n = N_n/N_{n-1}.$$

This estimator converges "almost surely" toward m as n tends to infinity. This is the strongest type of convergence for a random variable. It means that an estimate of m can be computed at each cycle. The random series of these estimates converges toward a limit that is the real value of the estimated parameter m.

We used this first estimator to build a second estimator for the initial copy number:

$$\hat{N}_{0,n} = N_n/\hat{m}_n^n.$$

The convergence of this estimator is not as strong as the convergence of $\hat{m}_n$. It is only a convergence almost sure to a random variable $W_{N_0,m}$. This means that the series $\hat{N}_{0,n}$ tends to a limit value as n tends to infinity, but this limit is not the real value of the estimated parameter N_0. The asymptotic value of this series is randomly distributed. All trajectories of $\hat{N}_{0,n}$ starting from the same initial conditions lead to different values. Thus, the limit of $\hat{N}_{0,n}$ computed on a trajectory of N_n is a realization of the random variable $W_{N_0,m}$. It is worth emphasizing that this random variable is a function of the amplification parameters N_0 and m. In particular, its expectation equals N_0, whereas its variance is $N_0 \cdot (2 - m)/m$. Last, we demonstrated that it has a probability density function defined on $[0, +\infty[$.

Because $\hat{N}_{0,n}$ does not converge to N_0, it would be helpful to assess the difference between N_0 and its estimation. A convenient way to express this discrepancy is to compute a confidence interval for N_0 on the basis of its estimation.

For technical reasons that are beyond the scope of this paper, the computation of the confidence interval requires us to normalize the estimation of N_0 so as to set its mean value to 0 and its variance to 1.

The computation of the N_0 confidence interval requires a set of critical values that will be used to limit the interval. The computation of the critical values is explained below. At this stage let us introduce the notations. So, let $w_1(m,\alpha)$, $w_2(m,\alpha)$ be the critical values used to compute the confidence interval of level α. With these notations the confi-

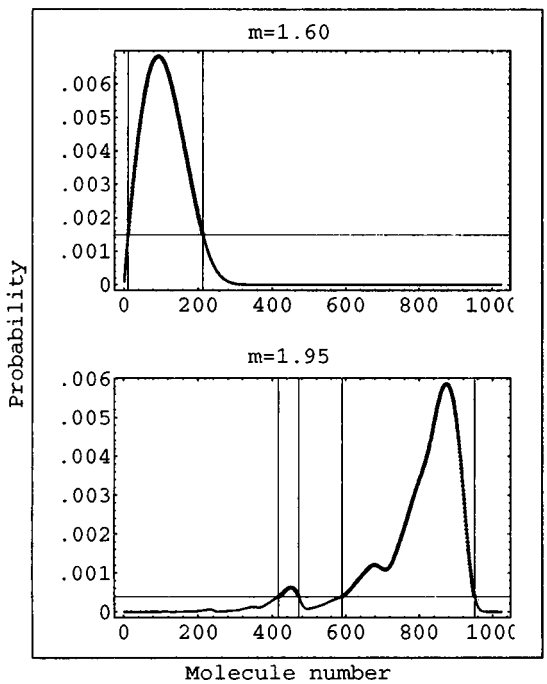

FIGURE 2 Effect of the amplification rate on the shape of N_{10} distribution. These two plots illustrate the influence of the amplification rate on the shape of the distribution of probability of N_n. It is interesting to note that for values of m greater than ~1.82, the distribution of probability is multimodal, as can be observed when $m = 1.95$. The general shape of this distribution is not influenced very much by the number of amplification cycles beyond cycle 10. Besides the effect of the amplification rate, the initial copy number has a major influence on the shape of the distribution, which tends to become gaussian as the initial copy number tends to infinity. The thick parts of the plots are the points inside the confidence area at the 5% level. They all have a probability greater than a threshold plotted by the horizontal line. The limits of the confidence area are represented by the vertical lines. In case of $m = 1.60$, the confidence area is a single interval, whereas for $m = 1.95$ the confidence region is the union of two intervals.

dence interval for N_0 is $[f_n^{-1}(w_2(m,\alpha)),\ f_n^{-1}(w_1(m,\alpha))]$ where $f_n^{-1}(x)$ is the inverse function of

$$f_n(x) = (\hat{N}_{0,n} - x) \cdot \left(x \frac{2 - \hat{m}_n}{\hat{m}_n}\right)^{-1/2}.$$

One can recognize the expectation and the standard deviation of $W_{N_0,m}$ in this expression. Actually, the probability that N_0 belongs to $[f_n^{-1}(w_2(m,\alpha)),\ f_n^{-1}(w_1(m,\alpha))]$ is not $1 - \alpha$, as it usually is for confidence intervals. Rather, when n tends to infinity, the probability that N_0 is inside this interval is greater than $1 - \alpha$. This is expressed by the formula

$$\lim_{n\to\infty} P(N_0 \in [f_n^{-1}(w_2(m,\alpha)), f_n^{-1}(w_1(m,\alpha))]) > 1 - \alpha.$$

The theoretical explanations have been deliberately limited to the minimum required to understand rest of the paper (Jacob and Peccoud, 1996a,b).

The implementation of this statistical analysis on a simulated set of data is reported in Fig. 1. The initial molecule number used in the simulation is 1 and the amplification is 1.8 up to and including cycle 25. Starting at cycle 26, the amplification rate looses 5% at each cycle up to cycle 30, when the amplification is stopped. The amplification rate estimates and the initial copy number estimates are plotted separately. The left plot is used to determine the ultimate cycle in the exponential phase of the reaction. This cycle can be determined either graphically or with a simple numerical criterion. Such a criterion was used here. Precisely, the convergence criterion is that three successive differences of $\hat{m}_n$ are less than a tolerance factor set to 10^{-2} in this analysis. The last cycle of this series is the end of the exponential phase. The magnitude of this tolerance factor is symbolized on the left plot by the thickness of the horizontal line. The vertical line is used to materialize the ultimate cycle of the exponential phase. The right plot makes very clear that the convergence of $\hat{N}_{0,n}$ is not as fast as that of $\hat{m}_n$. Thus, the best estimate of N_0 is the one computed at the last cycle of the exponential phase. The value of this estimate is reported on the axis by the horizontal line, whereas its confidence interval is materialized by the vertical bar.

EXPERIMENTAL EVIDENCE

This stochastic model of the PCR amplification seems to be consistent with data published by several authors. There is some evidence of large fluctuations of the final amount of amplified material when the initial molecule number is very low. The quantification of the plasma HIV-1 virion-associated RNA was attempted by reverse-transcription competitive PCR. Because the sensibility of the quantification protocol is essential for monitoring the infection, the authors determined its threshold sensitivity to be 100 copies. Positive signals could be detected for as few as 10 copies, but results were less consistent, and thus quantitation was less reliable (Piatak et al., 1993). Obviously, with these results randomness cannot be assigned solely to the PCR reaction. The other steps, such as liquid transfers or the reverse transcription, could also be responsible for the variance of the final result. However, in accordance with the results plotted in Fig. 2, we suspect that the amplification step itself is a major source of fluctuation for the final result of this experiment.

The same kind of observations is reported in a more recent paper (Lantz and Bendelac, 1994). This case fits better with our model. Cells were sorted in 96-well plates at one cell per well, and the DNA was amplified with a set of primer specific for a genomic rearrangement of the T-cell receptor genes. Quantitative results were individually recorded and displayed an amazing variability. Because the initial conditions of the PCR are homogeneous among positive cells, it is difficult to justify the 10-fold differences between the results by any other source of fluctuations. These data distributions even seem to be very irregular and to have several peaks. A rigorous statistical analysis of the goodness of fit to our theoretical distributions should be conducted to verify this hypothesis, but it is not immedi-

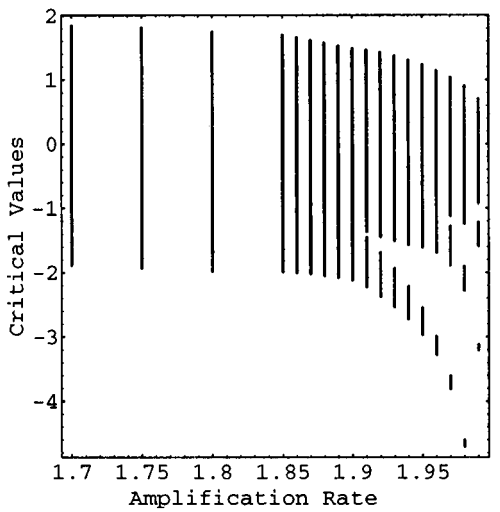

FIGURE 3 Critical values as a function of the amplification rate. In this figure, the confidence region is reported for $\alpha = 5\%$ and m ranging from 1.7 to 1.99. The confidence region is represented by vertical lines. This figure illustrates the influence of the amplification rate on the topology of the confidence region. For instance, one can observe that it is split for a value of m between 1.90 and 1.91. For m greater than 1.97, the confidence region is the union of three intervals. Note that the size of the confidence region is also under the control of m. It is particularly spectacular when m is close to 2, where it seems to collapse. This behavior is related to the fact that for $m = 2$ the distribution has null variance, because the process is then deterministic.

ately possible with the published data, because the amplifications were conducted beyond the exponential phase.

As far as we know, there is only one work that specifically addresses the question of large fluctuations of the final amount of amplification products when starting from a low number of copies (Karrer et al., 1995). Its authors named this phenomon the "Monte Carlo effect." Part of the observations reported in this paper are specifically devoted to demonstrating that this effect is not an artifact. However, here again it is not possible to analyze these data using our results, because the experiments involve serial dilutions that certainly introduce some extra variance in the final result.

Russ Higuchi kindly provided us the data produced by the prototype he engineered (Higuchi et al., 1993). This kind of data fits perfectly with our model, and we could proceed to the estimation of the amplification rate. Yet, it quickly appeared that the dynamic range of this prototype was not sufficient to allow recording of the data during the exponential phase. There was only a twofold difference between the background noise and the highest recorded signals. The computation of the amplification rate estimator allowed us to observe a smooth evolution similar to what happens to $\hat{m}_n$ after cycle 25 on Fig. 1. Since the publication of this paper, the prototype has been refined and has been released by Perkin-Elmer as the ABI PRISM 7700 Sequence Detector. The sensitivity of its data acquisition hardware has been enhanced, so that several points can be reliably recorded during the exponential phase. No data have been available so far, but the applicability of our results to the analysis of the data produced by this machine will be studied as soon as possible.

COMPUTATION OF CRITICAL VALUES

Whatever the initial copy number, the critical values $w_1(m,\alpha),w_2(m,\alpha)$ must be computed from the law of $W_{1,m}$ after normalization. Hence the computation of the distribution of N_n starting from $N_0 = 1$ was a priority.

A PCR amplification starting from a single copy DNA sequence leads to a random number of molecules after n cycles of amplification. Whatever the rate of amplification, the size of the population resulting from the amplification of the initial target sequence is between 1 and 2^n. The probability of each possible issue of an amplification can be computed analytically and numerically with a computer system with symbolic capabilities such as Mathematica (Wolfram Research, 1992). The generating function of the law of probability of the offspring number of a single molecule is $g(s) = (2 - m)s + (m - 1)s^2$. Branching processes have a useful property. The composition of the generating function over itself n times, $g^{(n)}(s) = g(g^{n-1)}(s))$, is the generating function of the law of the offspring number of a single molecule after n cycles of amplification. Thus, the coefficient of s^k is the probability of having k molecules after n cycles. This algorithm has been used to compute the frequencies of the two histograms plotted in Fig. 2.

The law of $W_{1,m}$ is derived from the law of N_n by dividing the values of N_n by m^n. In a similar way, we proceed to the normalization of $W_{1,m}$. The upper and lower bounds of the confidence interval of probability 0.95 were computed. To do this, the mode of the distribution of probability was used as a starting point. For each probability q between 0 and the probability of the mode, it is possible to compute the sum of the probabilities of the points having a probability greater than q. The set of points having a probability greater than q, such that its total probability is 0.95, is the confidence region of probability 0.95. Because the distribution of N_n is discrete, the approximation of the law of $W_{1,m}$ is also discrete. We can even compute the distance between two successive values:

$$\sqrt{\frac{m}{2-m}} \cdot m^{-n}.$$

For $m = 1.8$ and $n = 12$, this distance is 2.59×10^{-3}. Thus, proceeding to a local polynomial interpolation helps to refine the critical value estimation. This procedure was conducted with the distributions of N_{10}, N_{11}, N_{12}, N_{13} to check the convergence of these successive approximations of the critical values. The slight trend observed among them ensures that they are accurate to the second decimal (data not shown). It was not possible to compute other estimates for greater numbers of cycles, because these computations are very intensive. The generating function of the law of probability of N_n is a polynomial of degree 2^n. For $n = 13$, this means that polynomials of a degree greater than $8 \times$

10^3 were manipulated. For instance, the computation of the probability distribution of N_{13} took approximately 35 cpu minutes on a workstation based on an Alpha microprocessor.

Because for values of m greater than 1.82, the distribution of probability of N_n is multimodal (with several local maxima of probability), the above procedure may not lead to a single interval, but rather to a union of intervals (see Fig. 3). In this case each interval is limited by a pair of critical values. This is not an artifact. The procedure was actually designed to achieve this, because in this case this type of confidence region is more meaningful than any single confidence interval.

MONTE CARLO SIMULATIONS

Because the analytical results reported above are only asymptotic properties that hold when the number of cycles tends to infinity, it is necessary to appraise their validity when the number of cycles is finite. Two questions in particular require scrutiny. First, under which conditions of n, m, and N_0 is the variance of $\hat{m}_n$ negligible in the range of parameter values commonly used in laboratory practice? Second, under which conditions of n, m, and N_0 is the confidence interval for N_0 statistically valid?

The simulation algorithm is very easy to implement, because the distribution of N_n, given that $N_{n-1} = N$, is the binomial distribution with parameters N and p. When N_n was greater than 1000, the gaussian approximation of the binomial distribution was used. Simulations were performed with $m = 1.6$ and $m = 1.8$ and with $N_0 = 1$ and $N_0 = 1000$. For each of these sets of parameter values, 500 trajectories of the process were simulated up to cycle 30. The series of $\hat{m}_n$ and $\hat{N}_{0,n}$ were computed for each trajectory, as were the confidence intervals at the 5% level of N_0. The presence of N_0 inside this interval was checked for.

The best way to appreciate the proximity of the asymptotics is to carefully examine the dispersion of the two estimators. Thus in Table 1 we reported the mean value, the range (the difference between the two extreme values), the standard deviation, and the standard error (standard deviation $\times$ sample size$^{-1/2}$) of the two estimators over the 500 trajectories recorded. This table illustrates quite well the different kinds of convergence of $\hat{m}_n$ and $\hat{N}_{0,n}$. Because $\hat{m}_n$ almost surely converges to m, its mean value is extremely close to the actual rate of amplification and its dispersion indicators have extremely low values, which steadily decrease as n grows. Moreover, we observe that the convergence is faster when $N_0 = 1000$ and when $m = 1.8$. The first effect is a consequence of the central limit theorem when N_0 tends to infinity. The second is a direct consequence of the fact that the convergence speed is on the order of $m^{n/2}$. Because of its convergence to a random variable $W_{N_0,m}$ and not to N_0, the estimator $\hat{N}_{0,n}$ behaves differently. First, no trend can be noticed in its mean value. No accuracy is gained as the number of cycles grows. Here, the proximity to the asymptotics is not indicated by the low value of the dispersion indicators, but rather by comparing the standard deviation computed on the 500 trajectories to the standard deviation of $W_{N_0,m}$ denoted by σ_∞,

$$\sigma_\infty = (N_0(2 - m)/m)^{1/2}.$$

The numerical values of σ_∞ under the different conditions of simulation are reported in Table 1 to make the comparison easier. At cycle 10, the standard deviation is somewhat greater than σ_∞, whereas at cycles 20 and 30 it is approximately equal to σ_∞. Actually, it is even slightly smaller than σ_∞. This is not an artifact, because this is consistent with theoretical results, but these are beyond the scope of this article.

During the theoretical part of our work, we were unable to determine an exact level for the confidence interval and found only its upper boundary. The Monte Carlo simulations help estimate the real level of this confidence interval, with the frequency of confidence intervals not encompassing the initial number of molecules used to initiate the simulation. This frequency, denoted $\hat{\beta}$, is an estimator of β, which is the real level. Of course, $\beta \leq \alpha$. To appreciate the accuracy of the estimate of β computed on the data set collected during the simulation, we can compute a confidence interval for β. The length of this interval is the best indication of the estimate's precision. To avoid possible confusion, we want to emphasize explicitly that this confidence interval has nothing to do with the confidence interval of N_0 computed on each PCR trajectory. A classical formula found in textbooks (Wonnacott and Wonnacott, 1990) allows the computation of the β confidence interval:

$$P(\beta_{inf} \leq \beta \leq \beta_{sup}) \geq 0.95:$$

$$\hat{\beta} - \beta_{inf} = \beta_{sup} - \hat{\beta}$$

$$= 1.96(\hat{\beta}(1 - \hat{\beta})/\text{Sample size})^{1/2}.$$

The confidence intervals computed in the four simulation conditions are reported in Table 2. From this table it is possible to deduce that $\hat{\beta}$ is very close to 5% when $N_0 = 1000$, whereas it is approximately 2% when $N_0 = 1$.

MEASUREMENT UNCERTAINTIES

The conditions under which our theoretical results can be applied to experimental data have been clarified by the

TABLE 2 Proportion of N_0 confidence intervals at level α = 5% that do not contain N_0 at cycle 30

	β_{inf}	$\hat{\beta}$	β_{sup}
$N_0 = 1$			
$m = 1.6$	0.0091	0.0220	0.0348
$m = 1.8$	0.0077	0.0200	0.0322
$N_0 = 1000$			
$m = 1.6$	0.0276	0.0460	0.0643
$m = 1.8$	0.0292	0.0480	0.0667

Monte Carlo simulations. So they can be used to evaluate the potential of Q-PCR as a quantification method. Several different words are used, sometimes in a confused manner, to express the quality of a measurement. The accuracy of a measurement is the close agreement between the result of a measurement and the true value of the measurand. It includes some combination of both precision and bias. The bias is the offset of a group of measurements from the true value. The precision is the dispersion of the measurements. A better term than "accuracy" is "uncertainty of measurement," which states the expected range of values for a measurement and includes all sources of uncertainty, i.e., both the precision and the bias. "Uncertainty" is easier to use because a low numeric value of uncertainty corresponds to a low uncertainty, whereas a low numeric value of accuracy corresponds to a high accuracy, which may create confusion. The International Organization for Standardization and the National Conference of Standards Laboratories provide very helpful documents covering these topics (International Organization for Standardization, 1993; National Conference of Standard Laboratories, 1994). A rigorous definition would be that the amplitude of the confidence interval of N_0 is the expanded uncertainty of the measurement, but because we do not refer to other type of uncertainty, we will simply use the term "uncertainty."

We can evaluate the inherent uncertainty of PCR as a quantification principle. This uncertainty is plotted in Fig. 4 for five different rates of amplification and for an initial molecule number ranging from 1 to 100. For a low initial number close to unity, the relative uncertainty (ratio of uncertainty over true value) is greater than 100%. For instance, the confidence interval computed with $N_0 = 1$ and $m = 1.5$ is [0.344, 2.901]. This means that in this case the relative uncertainty is 255%, because the amplitude of the confidence interval is 2.55. This example is the most extreme case considered in this paper, because N_0 has been set to its lowest possible value and because the critical values have not been computed for amplification rates below 1.5. A second example can help to illustrate that high rates of amplification can significantly reduce uncertainty when N_0 is close to unity. The confidence interval computed with $N_0 = 1$ and $m = 1.9$ is [0.606, 1.597]. Here, the relative uncertainty is only 99.1%. The uncertainty also decreases quickly as the initial number of molecules N_0 grows. For N_0 close to 100, the relative uncertainty ranges between 10 and 25%, depending on the amplification rate. Those values are not negligible. Of course, for larger initial quantities the uncertainty would be smaller. For instance, a relative uncertainty of 1% is achieved for $N_0 = 10^4$ and $m = 1.88$.

It is not surprising then that large fluctuations are observed when quantifications of minute quantities of target molecules are attempted. A comparison of these experimental fluctuations to the theoretical uncertainty computed in this paper would be of great value. The uncertainty of a real experimental measurement is naturally greater than the uncertainty of its simulated counterpart. The nucleic acid extraction, the reverse transcription, or the quantification steps all propagate their own uncertainty in the final result. As soon as a device is available to conduct the experiment modeled in this paper, it would be interesting to calibrate it precisely so as to achieve the error propagation analysis with real data. The limit of reliability of Q-PCR is recognized to be higher than the detection sensitivity of the PCR itself. We hope that our results will contribute to the extension of the use of PCR to quantify small numbers of target molecules by clarifying the intrinsic fluctuations of the reaction and providing algorithms to cope with it.

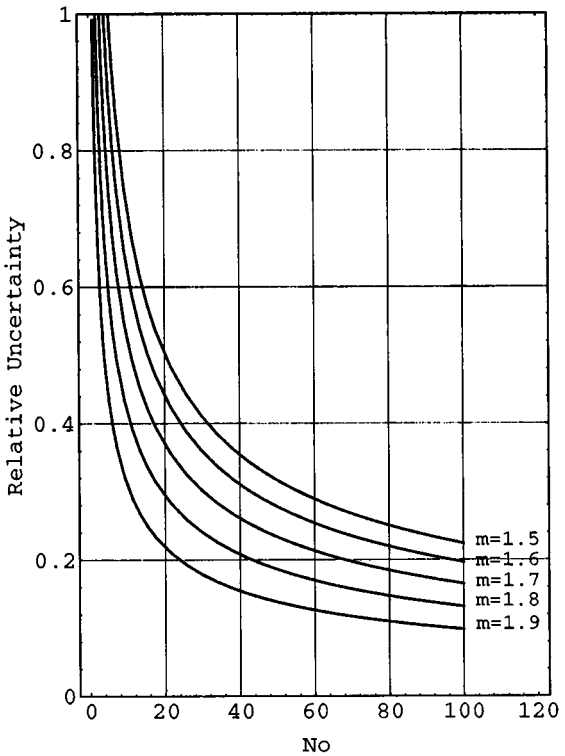

FIGURE 4 Initial molecule number and rate of amplification influence on the relative uncertainty of Q-PCR. The amplitude of the confidence interval of N_0 divided by N_0 can be regarded as an expression of the relative uncertainty of a quantification protocol based on a PCR amplification. On this plot, it is possible to note both the effect of the amplification rate on this precision index and the effect of the initial number of target molecules. This latter parameter has the most significant effect. When the initial molecule number is 100, the relative uncertainty is between 10% and 25%, depending on the amplification rate. This illustrates that even for relatively large numbers of target molecules, the fluctuations are not negligible.

Note added in proof: All of the computations reported in this paper have been done with Mathematica (Wolfram Research, 1992). The whole set of packages as well as documenting notebooks are available through anonymous FTP at ftp.imag.fr in/pub/TIMC/TIMB.

We are indebted to Pr. Jacques Demongeot for his constant encouragement in the process of writing this paper, and to Dr. Philippe Dumas for very stimulating discussions in the early phase of this work. Special thanks to Mark Maxwell from McDonnell Douglas Aerospace for introducing us to the proper vocabulary of metrology. We thank Ms. Kate Wright for reading and correcting the English version of the manuscript.

JP is supported by INSERM and CJ by INRA.

REFERENCES

Cui, X. F., T. M. Goradia, K. Lange, and H. H. Kazazian Jr. 1989. Single-sperm typing: determination of genetic distance between the Gg-globin gene and parathyroid hormone loci by using the polymerase chain reaction and allele specific oligomers. *Proc. Natl. Acad. Sci. USA.* 86:9389–9393.

Erdi, P., and J. Toth. 1989. Mathematical Models of the Chemical Reaction. Manchester University Press, Manchester, England.

Erlich, H. A., D. Gelfand, and J. J. Sninsky. 1991. Recent advances in the polymerase chain reaction. *Science.* 252:1643–1651.

Ferre, F., A. Marchese, P. Pezzoli, S. Griffin, E. Buxton, and V. Boyer. 1994. Quantitative PCR—an overview. *In* The Polymerase Chain Reaction. K. B. Mullis, F. Ferre, and R. A. Gibbs, editors. Birkhäuser, Cambridge, MA. 67–88.

Guttorp, P. 1991. Statistical Inference for Branching Processes. John Wiley and Sons, New York.

Higuchi, R., C. Fockler, G. Dollinger, and R. Watson. 1993. Kinetic PCR analysis: real-time monitoring of DNA amplification reactions. *Biotechnology.* 11:1026–1030.

Hoof, T., J. R. Riordan, and B. Tummler. 1991. Quantitation of mRNA by the kinetic polymerase chain reaction assay: a tool for monitoring P-glycoprotein gene expression. *Anal. Biochem.* 196:161–169.

International Organization for Standardization. 1993. Guide to the Expression of Uncertainty in Measurement. ISO, Geneva.

Jacob, C., and J. Peccoud. 1996a. Inference on the initial size of a supercritical branching process from partial and migrating observations. *C. R. Acad. Sci. Paris Ser. I.* 322:875–880.

Jacob, C., and J. Peccoud. 1996b. Estimation of the offspring mean for a supercritical branching process from partial and migrating observations. *C. R. Acad. Sci. Paris Ser. I.* 322:763–768.

Karrer, E. E., J. E. Lincoln, S. Hogenhout, A. B. Bennett, R. M. Bostock, B. Martineau, W. J. Lucas, D. G. Gilchrist, and D. Alexander. 1995. In situ isolation of mRNA from individual plant cells: creation of cell-specific cDNA libraries. *Proc. Natl. Acad. Sci. USA.* 92:3814–3818.

Krawczak, M., J. Reiss, J. Schmidtke, and U. Rosler. 1989. Polymerase chain reaction: replication errors and reliability of gene diagnosis. *Nucleic Acids Res.* 17:2197–2201.

Lantz, O., and A. Bendelac. 1994. An invariant T cell receptor alpha chain is used by a unique subset of major histocompatibility complex class I-specific CD4+ and CD4-CD8− T cells in mice and humans. *J. Exp. Med.* 180:1097–1106.

Li, H. H., U. B. Gyllensten, X. F. Cui, R. K. Saiki, H. A. Erlich, and N. Arnheim. 1988. Amplification and analysis of DNA sequences in single human sperm and diploid cells. *Nature.* 335:414–417.

Lion, T., T. Henn, A. Gaiger, P. Kalhs, and H. Gadner. 1993. Early detection of relapse after bone marrow transplantation in patients with chronic myelogenous leukaemia. *Lancet.* 341:275–276.

Mullis, K. B., F. Ferre, and R. A. Gibbs. 1994. The Polymerase Chain Reaction. Birkhäuser, Cambridge, MA.

National Conference of Standard Laboratories. 1994. Determining and Reporting Measurement Uncertainties, RP-12. NCSL, Boulder, CO.

Nedelman, J., P. Heagerty, and C. Lawrence. 1992a. Quantitative PCR: procedures and precision. *Bull. Math. Biol.* 54:477–502.

Nedelman, J., P. Heagerty, and C. Lawrence. 1992b. Quantitative PCR with internal controls. *Comput. Appl. Biosci.* 8:65–70.

Piatak, M., M. S. Saag, L. C. Yang, S. J. Clark, J. C. Kappes, K. C. Luk, B. H. Hahn, G. M. Shaw, and J. D. Lifson. 1993. High levels of HIV-1 in plasma during all stages of infection determined by competitive PCR. *Science.* 259:1749–1754.

Raeymaekers, L. 1993. Quantitative PCR—theoretical considerations with practical implications. *Anal. Biochem.* 214:582–585.

Raeymaekers, L. 1994. Comments on quantitative PCR. *Eur. Cytokine Netw.* 5:57.

Santagati, S., E. Bettini, M. Asdente, M. Muramatsu, and A. Maggi. 1993. Theoretical considerations for the application of competitive polymerase chain reaction to the quantitation of a low abundance messenger RNA-estrogen receptor. *Biochem. Pharmacol.* 46:1797–1803.

Semple, M. G., S. Kaye, C. Loveday, and R. S. Tedder. 1993. HIV-1 plasma viraemia quantification—a non-culture measurement needed for therapeutic trials. *J. Virol. Methods.* 41:167–179.

Shire, D. 1994. Quantitative PCR: reply. *Eur. Cytokine Netw.* 5:59–60.

Simmonds, P., L. Q. Zhang, H. G. Watson, S. Rebus, E. D. Ferguson, P. Balfe, G. H. Leadbetter, P. L. Yap, J. F. Peutherer, and C. A. Ludlam. 1990. Hepatitis C quantification and sequencing in blood products, haemophiliacs, and drug users. *Lancet.* 336:1469–1472.

Singer-Sam, J., V. Chapman, J. M. Le Bon, and A. D. Riggs. 1992. Parental imprinting studied by allele-specific primer extension after PCR: paternal X chromosome-linked genes are transcribed prior to preferential paternal X chromosome inactivation. *Proc. Natl. Acad. Sci. USA.* 89:10469–10473.

Snabes, M. C., S. S. Chong, S. B. Subramanian, K. Kristjansson, D. Disepio, and M. R. Hughes. 1994. Preimplantation single-cell analysis of multiple genetic loci by whole-genome amplification. *Proc. Natl. Acad. Sci. USA.* 91:6181–6185.

Wang, A. M., M. V. Doyle, and D. F. Mark. 1989. Quantitation of mRNA by the polymerase chain reaction. *Proc. Natl. Acad. Sci. USA.* 86: 9717–9721.

Wiesner, R. J., B. Beinbrech, and J. C. Ruegg. 1993. Quantitative PCR. *Nature.* 366:416.

Wiesner, R. J., J. C. Ruegg, and I. Morano. 1992. Counting target molecules by exponential polymerase chain reaction: copy number of mitochondrial DNA in rat tissues. *Biochem. Biophys. Res. Commun.* 183:553–559.

Wolfram Research. 1992. Mathematica. Wolfram Research, Champaign, IL.

Wonnacott, T. H., and R. J. Wonnacott. 1990. Introductory Statistics for Business and Economics. John Wiley and Sons, New York.

Wood, R., H. Dong, D. A. Katzenstein, and T. C. Merigan. 1993. Quantification and comparison of HIV-1 proviral load in peripheral blood mononuclear cells and isolated CD4+ T cells. *J. Acquir. Immune Defic. Syndr.* 6:237–240.

Zhang, L., C. Xiangfeng, K. Schmitt, and R. Hubert. 1992. Whole genome amplification from a single cell: implications for genetic analysis. *Proc. Natl. Acad. Sci. USA.* 89:5847–5851.